Research highlight

Mohan Leena, Shanmugam Srinivasan* and Marimuthu Prabhaharan

Evaluation of acoustical parameters and thermal conductivity of TiO_2-ethylene glycol nanofluid using ultrasonic velocity measurements

DOI 10.1515/ntrev-2015-0016
Received March 9, 2015; accepted July 16, 2015; previously published online September 1, 2015

Abstract: The nanosized titanium oxide (TiO_2) nanoparticles (NPs) were synthesized via sol-gel method. The crystalline nature of the synthesized TiO_2 nanoparticles was confirmed by X-ray powder diffractometry method. The surface morphology and particle size of the nanoparticles were analyzed by high-resolution scanning electron microscopic method. UV-visible spectroscopy was employed to determine its band gap energy value. The different concentrations of nanofluid samples of TiO_2 NPs dispersed in ethylene glycol were prepared and mixed thoroughly by ultrasonication process. The value of ultrasonic velocity and density were measured for the different concentrations of TiO_2 nanofluids. The acoustical parameters such as adiabatic compressibility, intermolecular free length, and acoustic impedance were calculated from the experimental data. It was observed that ultrasonic velocity showed linearity with particle concentration, and the results were discussed. In addition to the TiO_2-ethylene glycol (particle-fluid) interaction studies, a new methodology was proposed to find the thermal conductivity of nanofluids using ultrasonic velocity.

Keywords: ethylene glycol (EG); nanofluids; thermal conductivity; TiO_2; ultrasonic velocity.

***Corresponding author: Shanmugam Srinivasan,** Department of Physics, Presidency College (Autonomous), Chennai 600 005, India, e-mail: dr_s_srinivasan@yahoo.com
Mohan Leena: Department of Physics, Presidency College (Autonomous), Chennai 600 005, India
Marimuthu Prabhaharan: Department of Physics, Aksheyaa College of Engineering, Puludivakkam, Kanchepuram-Dt. 603 314, India

1 Introduction

It is a well-known fact that by tuning the size of the particle, one could transform the property of the material and make use of it in different applications. The suspensions of nanoparticles in a base fluid called nanofluids could provide dramatic improvements concerning the heat transfer properties of host fluids. There is a great interest toward nanofluids due to their enhanced thermal conductivity compared with bulk fluids. The nanofluids find wide applications in the field of electronics, transportation, medicine, solar cells, sensors, cooling, MEMS, tunable optical fiber, optical switches, etc. [1–6]. Nanofluids provide a new cooling and also an optimistic outlook in improving the efficiency of heat transfer rate. A high efficiency of heat transfer could be obtained with the nanofluids containing NPs of higher thermal conductivity [7, 8]. A scan of the literature survey revealed that numerous works have enhanced the thermal conductivity of suspensions that contained the solid particles since Maxwell's theoretical work was published more than 100 years ago [9–13]. The metal oxide NPs are preferred for preparing nanofluids, though it possesses low heat transfer capacities than metals [14–24]. Metal nanoparticles increase the interfacial resistance due to the surface oxidation, and hence, its thermal conductivity decreases. The metal oxide-based nanofluids find a promising place in the list of potential nanofluid systems. They are less hazardous than metal nanoparticles, and also, they surpass the possible reduction in thermal conductivity on account of interfacial resistance.

Ultrasonic measurement has become a powerful tool in studying the physicochemical properties of matter [25–27]. Measurement of ultrasonic velocity and other derived parameters in the solvent plays essentially a vital role in the study of molecular interactions between the solute and solvent systems. TiO_2 NPs are one of the promising n-type semiconductors that have many attractive properties including high refractive index, high dielectric constant, chemical stability, and a wider band gap. The low freezing

point, high boiling point, and moderate heat transfer properties of ethylene glycol motivated us to choose it as the base fluid. In the present study, the ultrasonic velocity measurement of the TiO_2-EG nanofluids has been measured to know how they interact with each other. Also, we intended to formulate the relationship between ultrasonic velocity and thermal conductivity of nanofluids, which would be of great importance in view of the difficulties in the experimental determination of thermal conductivities of a fluid system.

2 Materials and methods

2.1 Synthesis and characterization

The TiO_2 NPs were prepared via sol-gel method using Titanium (IV) isopropoxide (TTIP) as a precursor obtained from Sigma Aldrich Company, USA with a stated purity of 97%. TTIP was dropped slowly into the mixed solution of ethanol and distilled water (Merck, Germany) in the stoichiometry ratio of 1:4:1 (TTIP/H_2O/ethanol). The solution was continuously stirred to obtain a white slurry solution for 1 h at room temperature. Nitric acid (Merck, Germany) was used to adjust the pH in the range 2–3. The mixture was dried at 120°C for 2 h to evaporate water and other waste organic material. Finally, the dried powder was sintered at 450°C for 2 h to obtain the TiO_2 nanopowder.

The synthesized TiO_2 NPs were dispersed in EG (Merck, Germany) by employing ultrasonication for 3 h to get a homogenous suspension without any phase separation and sedimentation. It has been noticed that the ultrasonication increases the stability of the suspension. Nanofluids of various concentrations (0.04, 0.05, 0.06, 0.07, 0.08, 0.09, 0.1, and 0.2 wt.%) were prepared without the addition of any surfactant. No surfactant has been used in order to avoid its effects on the surface property of the nanoparticle and also to avoid chemical contamination. The synthesized TiO_2-EG nanofluids of various concentrations are shown in Figure 1.

The crystalline structure, phase composition, and average crystallite size of TiO_2 NPs have been identified from the X-ray diffraction patterns obtained using 3000 TT X-ray diffractometer (Serifert Co., Germany) at 293 K, operating at 30 kV and 30 mA with Cu-Kα radiation (λ=1.541 Å) for 2θ value ranging from 10° to 80°. The average particle size and morphology of TiO_2 nanoparticles have been examined using a High Resolution Scanning Electron Microscope (QUNTA FEG 200, FEI Company, Netherland). The digital ultrasonicator (LMCU-2A: 50 W, 40 KHz, Labman Scientific Instruments Pvt. Ltd., Chennai, India) energy is being produced by converting electrical energy into mechanical vibrations by using generator and piezoelectric transducers. UV-visible spectra of the samples have been dispersed in EG under ultrasonication, recorded on a T90+UV-VIS spectrometer (PG Instruments Ltd., Leicester, UK). The values of the band gap energy have been calculated for the different concentrations of TiO_2 nanofluids, and its stability analysis was done with the UV-visible spectrum measurements.

The density was determined using a specific gravity bottle by the relative measurement method. The weight of the sample was measured using the electronic digital balance with an accuracy of ±0.1 mg (Model: ELB 300, Shimadzu Corporation, Japan). The ultrasonic velocity of a pure solvent and their solutions have been measured by using digital ultrasonic interferometer operating at 2 MHz (Model: VCT 70A, Vi microsystem Pvt. Ltd., Chennai, India). The uncertainty was estimated to be 1 ms^{-1}. All the measurements were carried out at 298.15 K and 1 atmospheric pressure. The uncertainty of the temperature is 0.1 K and that of the concentration was 0.0001 g cm^{-3}. The velocity and density measurements were repeated several times for accuracy. The errors between experimental values of density and ultrasonic velocity of EG were very close to that of the literature values [28].

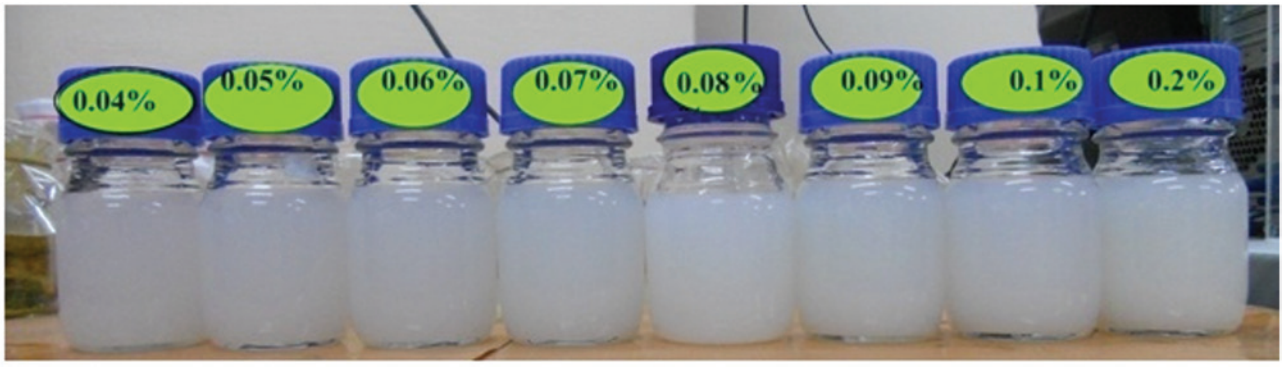

Figure 1: The photographic view of TiO_2 NPs in ethylene glycol.

From the experimental data of density and ultrasonic velocity of pure solvent and solutions, various acoustical parameters have been calculated using the following standard equations:

(i) Adiabatic compressibility $\beta=\frac{1}{U^2\rho}$

(ii) Free length $L_f=K\beta^{1/2}$

(iii) Acoustic impendence $Z=U\rho$

where β, U, ρ, L_f, K, and Z are the adiabatic compressibility, ultrasonic velocity, density, free length, temperature-dependent constant, and acoustic impedance of the solution, respectively.

3 Results and discussion

3.1 Structural and morphology studies

The crystal structure of the obtained powder was characterized by powder X-ray diffraction (XRD) analysis. From Figure 2, the highest peak at 25.4° (101), which was indicated as (101) plane anatase phase of TiO_2 pattern and matched well to the Joint Committee on Powder Diffraction Standards data (JCPDS, card no: 21-1272). The pattern confirms its tetragonal (4/m 2/m 2/m) crystal structure with lattice parameters of a=3.7845 Å, b=3.7845 Å, c=9.5143 Å, $\alpha=\beta=\gamma=90°$. The crystalline size obtained from the Scherrer formula is 34 nm. The morphology of the prepared TiO_2 sample was analyzed by HR-SEM, and it is shown in Figure 3. From the HR-SEM image, it has been observed that the synthesized TiO_2 NPs have an average size of 15 nm.

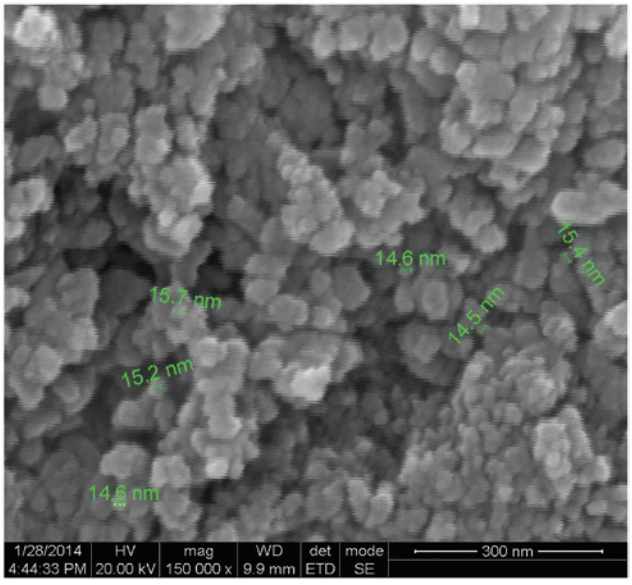

Figure 3: HR-SEM morphology of calcinated TiO_2 NPs at 450°C.

Energy dispersive X-ray spectroscopy (EDS) is an analytical technique used for the elemental analysis or chemical composition of a sample. The EDS spectrum of TiO_2 NPs is shown in Figure 4. It has been noticed that there was no trace of any other impurities within the detection limit of the EDS.

3.2 UV-visible spectral studies

The optical absorbance coefficient α of a semiconductor close to the band edge could be expressed by the following equation:

$$\alpha h\upsilon = A(h\upsilon - E_g)^n$$

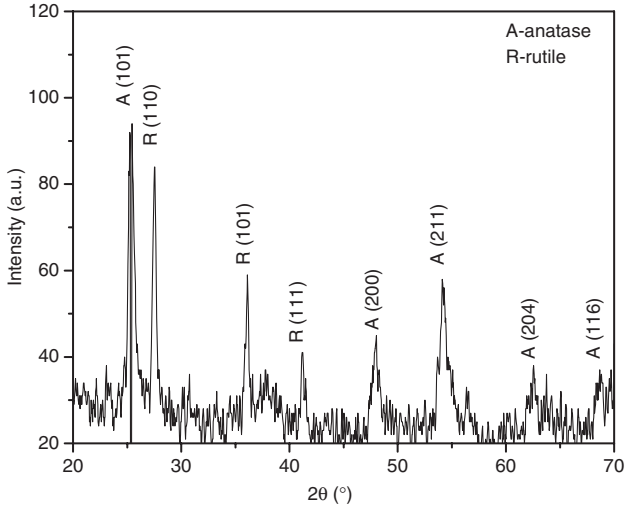

Figure 2: XRD Pattern of TiO_2 NPs sintered at 450°C.

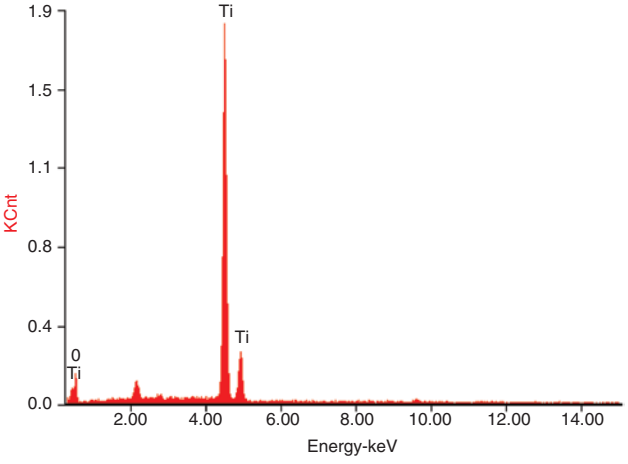

Figure 4: Energy dispersive X-ray spectrometry (EDS) of TiO_2 NPs.

where α is the optical absorption coefficient, E_g is the absorption band gap, A is a constant, n depends upon the nature of the transitions, n may have values 1/2, 2, 3/2, and 3 corresponding to allowed direct, allowed indirect, forbidden direct, and forbidden indirect transitions, respectively. In this case, n=1/2 for direct allowed transition [29].

The absorption spectra of TiO_2 NPs are shown in Figure 5A. The absorption band edges were estimated around 337, 343, 347, 350, 352, 360, 366, and 389 nm (about 3.68, 3.7, 3.61, 3.55, 3.5, 3.4, 3.37, and 3.2 eV).

The band gap of the energy could be determined by extrapolation to the zero coefficients, which has been

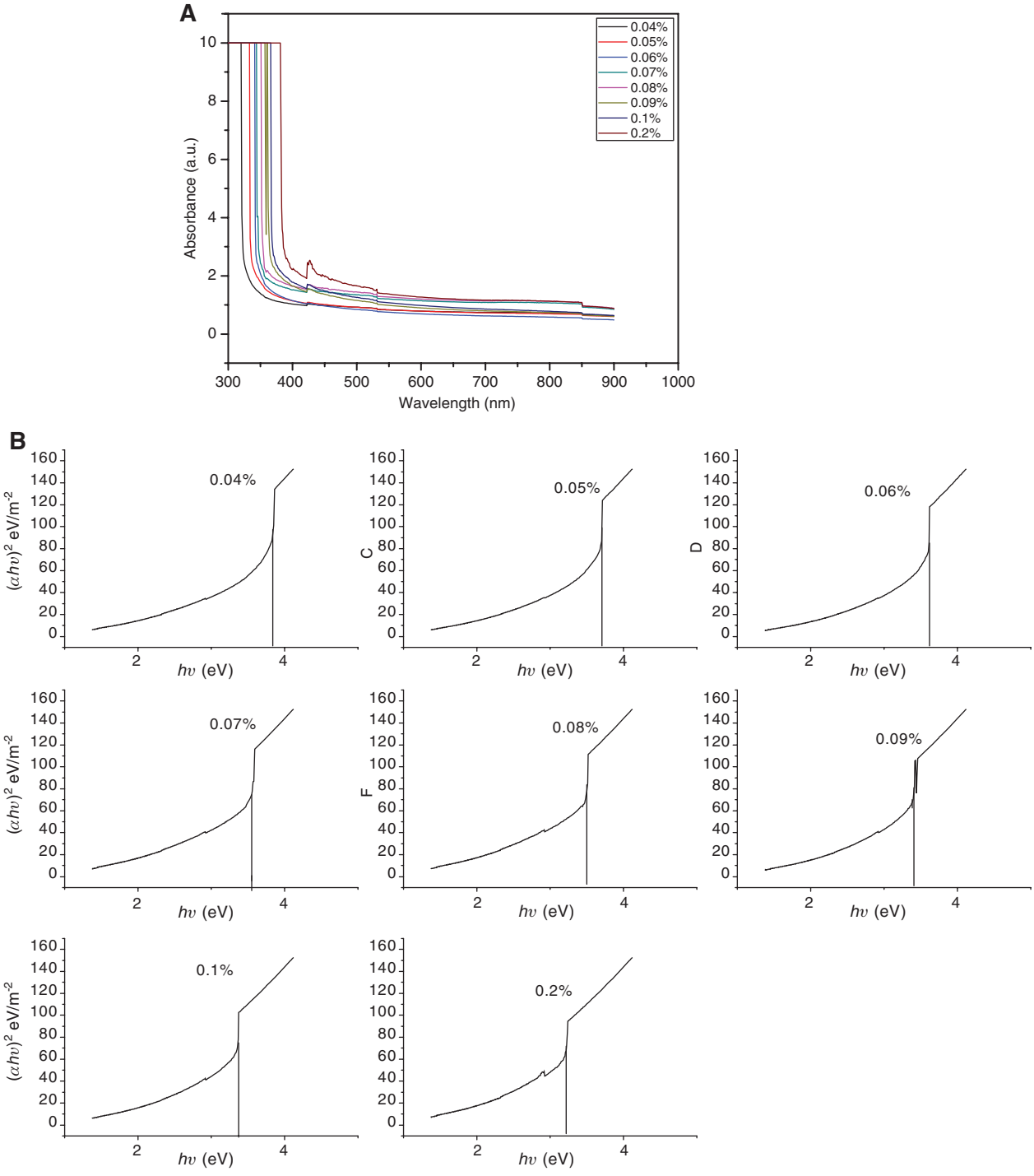

Figure 5: (A) UV-visible absorbance for TiO_2-ethylene glycol nanofluids. (B) Band gap obtained by extrapolating the linear portion of the $(\alpha h\upsilon)^2$ vs. $h\upsilon$ curve.

calculated from the above equation. The intercept of the tangent to the plot $(\alpha h\nu)^2$ vs. $h\nu$ in Figure 5B gives a good approximation of the band gap energy for this direct band gap of material. The band gap energies (E_g) of the as-prepared TiO_2 NPs are larger than the value of 3.2 eV for the bulk TiO_2. This could be explained as the band gap of the semiconductors has been found to be dependent on the particle size [30]. The band gap increases with a decreasing particle size, and the absorption edge has been shifted to a higher energy (blue shift) with that of the decreasing particle size. Considering the blue shift of the position of absorption, the bulk TiO_2, the absorption onset of the present samples could be assigned to the direct transition of electrons in the TiO_2 nanocrystals. The values of the band gap validate our crystallite size results according to the smaller crystallite size, which should have been a larger band gap (15 nm, 3.8 eV), and the large crystallite size should have a smaller band gap (15 nm, 3.7, 3.61, 3.55, 3.5, 3.4, 3.37, and 3.2 eV) by increasing and with the increase in concentration of the nanofluid.

In this paper, a brief study regarding dispersion stability has been made with the help of a UV-visible spectrometer. TiO_2 NPs have high UV light absorption characteristics. The stability of the fluids observed in terms of settling time is presented in the Table 1. The nanofluids have been found to be stable for more than 4 days with no sedimentation or phase separation. Hence, the absorbance of the sample was obtained at 390 nm every day and is plotted in Figure 6. It remains constant for up to 4 days (0.2 wt.%) from synthesis, and then starts decreasing, which ensures the stability of the nanofluid for more than 4 days.

3.3 Ultrasonic velocity studies

The velocity of ultrasound is the most significant parameter, and it is the quantum of molecular vibration in the medium through which the wave passes. It gives a quantitative measure of interparticle and intermolecular

Table 1: Stability of TiO_2-ethylene glycol nanofluids.

Sample no.	Concentration (wt.%)	Stability
1	0.04	5 days 22 h
2	0.05	5 days 13 h
3	0.06	5 days 06 h
4	0.07	5 days 01 h
5	0.08	4 days 20 h
6	0.09	4 days 14 h
7	0.10	4 days 08 h
8	0.20	4 days 00 h

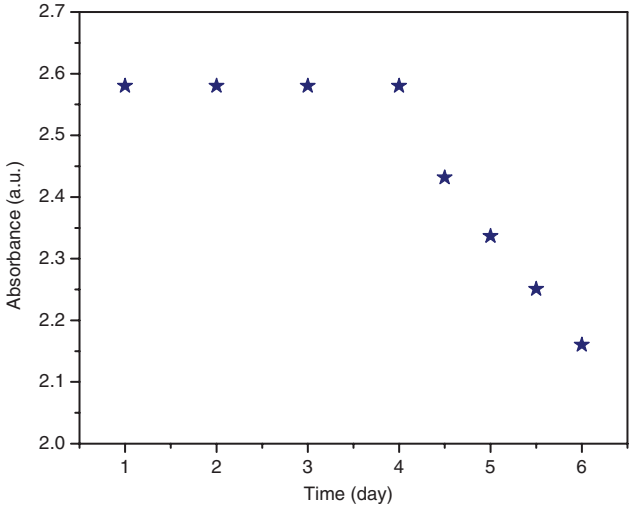

Figure 6: Plot of absorbance vs. time recorded at 390 nm.

interactions in the nanofluid sample, in their natural environment, without any dilution. The variation of the ultrasonic velocity with concentration is shown in Figure 7 where it is clear that the velocity of the nanofluid

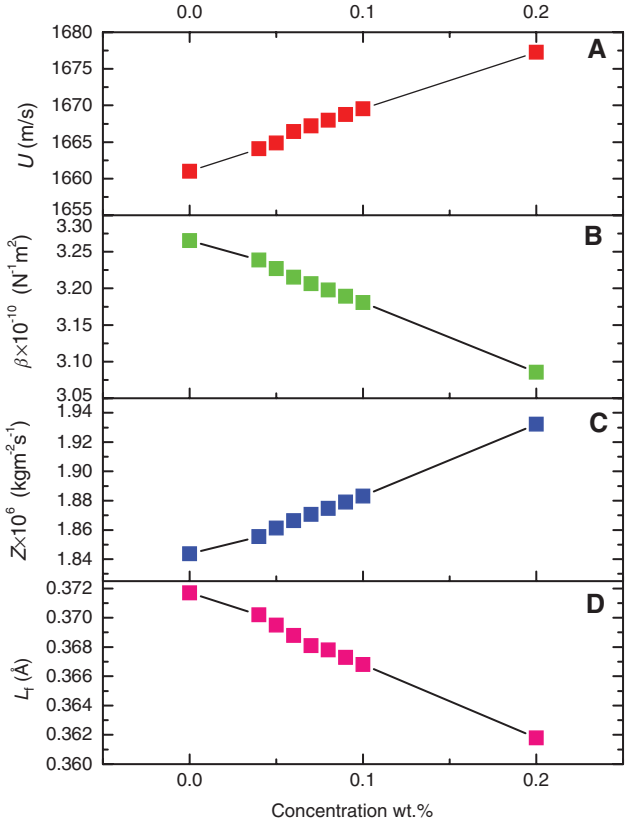

Figure 7: Acoustical parameters of TiO_2-NPs in ethylene glycol at different concentrations. (A) Ultrasonic velocity (U); (B) adiabatic compressibility (β); (C) acoustic impedance (Z); (D) free length (L_f).

increases with the increase in nanoparticle concentration. The velocity increases from 0.04 wt.% (for 0.036 vol.%) to 0.2 wt.% (for 0.18 vol.%), higher than that of the base fluid at 298.15 K. This enhancement in ultrasonic velocity with the increase in concentration has been attributed to the TiO_2-EG interactions, and it further ensures the dominance of intramolecular interaction over the intermolecular interactions [31]. Moreover, with the particle loading, there was a possibility of increasing the rate occurrence of the Brownian motion of the fluid molecule, along with the increase in surface layer that can persuade an increase in ultrasonic velocity.

As the structural changes affected the compressibility, there was a change in ultrasonic velocity. It was found that there was an increase in acoustic impedance values with an increase in the concentration of particles. Acoustic impedance is almost reciprocal to adiabatic compressibility. The higher value of the acoustic impedance indicates that there is a significant interaction between the particle and base fluid molecules, which might affect the structural arrangement. The interaction between the particles and the base fluid molecules increases the intermolecular distance between the molecules, which in turn causes impedance in the propagation of ultrasonic waves. The decrease in adiabatic compressibility and free length supports the particle and fluid interaction as shown by the ultrasonic velocity and acoustic impedance results. The calculated acoustical parameters are given in Table 2. The variations of ultrasonic velocity, free length, and acoustic impedance with TiO_2 nanofluid are illustrated in Figure 7.

3.4 Thermal conductivity studies

Thermal conductivity values k_{exp} of TiO_2-EG nanofluids of various concentrations measured at 298.15 K are depicted in Figure 8. The thermal conductivity of EG at 298.15 K was found to be 0.252 W/m K, which is in agreement with the value reported earlier [32]. The effective thermal conductivity of EG has been increased due to the addition of NPs. The increase in the thermal conductivity was proportional to the increase in particle concentration. Figure 8 represents the increase in thermal conductivity of EG due to the addition of NPs. The increase in thermal conductivity was attributed to the fact that the thermal conductivities of metal oxides are several orders of magnitude higher than those of liquids used as base fluids. It was observed that the nanofluid of 0.2 wt.% shows the maximum enhancement of 36.77% than the base fluid. The enhancement in thermal conductivity with nanoparticle loading in the nanofluid has been contributed by various factors such as Brownian motion, micro convection, clustering, and agglomeration [33, 34]. It is vivid from Figure 8 that the thermal conductivity of TiO_2-EG increases from 0.3374 to 0.3474 W/m K with respect to the increase in concentration from 0.04 to 0.2 wt.% with an enhancement of 2.96%.

One of the widely accepted trends in the theory of heat conduction of liquids is based on Debye's concept. As per Debye [35], the hydroacoustic vibrations (phonons) of a continuous medium (base fluid) are responsible for the heat transfer in liquids. Based on the above heat transfer mechanism, Bridgman has obtained a formula [36], characterized by the direct proportionality between thermal conductivity and from the assumption of the liquid state as a cubic lattice in which molecules have been arranged with minimal distance between their centers and is given by

$$k = 3\left(\frac{\rho N_A}{M}\right)^{2/3} k_B U \tag{1}$$

where N_A is the Avogadro's number, U is the velocity of the liquid, ρ is the density of the liquid, M is the molar mass of the liquid, and k_B, the Boltzmann's constant. The above

Table 2: Acoustical parameters of TiO_2 NPs in ethylene glycol.

Sample no.	Concentration of TiO_2 (wt.%)	Density (ρ) (kg m^{-3})	Ultrasonic velocity (U) (ms^{-1})	Adiabatic compressibility (β) (10^{-10} N^{-1} m^2)	Acoustic impedance (Z) (10^6 kg m^{-2} s^{-1})	Free length (L_f) (Å)
1	0.00	1110	1661.010	3.2654	1.8437	0.3717
2	0.04	1115	1664.099	3.2387	1.8555	0.3702
3	0.05	1118	1664.873	3.2270	1.8613	0.3695
4	0.06	1120	1666.424	3.2152	1.8664	0.3688
5	0.07	1122	1667.200	3.2065	1.8706	0.3681
6	0.08	1124	1668.977	3.1978	1.8748	0.3678
7	0.09	1126	1668.849	3.1892	1.8790	0.3673
8	0.10	1128	1649.528	3.1805	1.8832	0.3668
9	0.20	1152	1677.268	3.0856	1.9322	0.3613

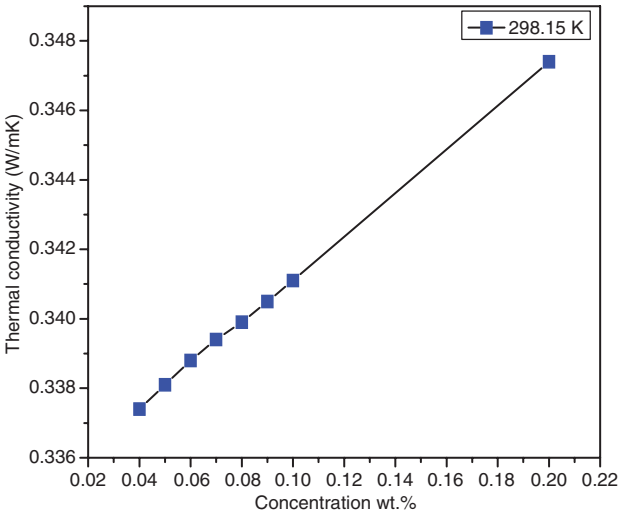

Figure 8: Thermal conductivity (k_{bm}) values obtained through the Bridgman equation.

equation is well established [35] for predicting the thermal conductivity of plain fluids used in the present work and to find the k value of EG. As there has been no effort reported, so far, in applying this equation to find out the thermal conductivity of nanofluids, it has been proposed to extend the equation to nanofluids. So, Eq. (1) is being modified by replacing the density and molar mass of a single liquid by those of nanofluids and is given in Eq. (2),

$$k_{bm} = 3\left(\frac{\rho_{nf} N_A}{M_{nf}}\right)^{2/3} k_B U \tag{2}$$

where k_{bm} is the thermal conductivity value obtained through the modified Bridgman equation, U is the velocity of the nanofluid, ρ_{nf} is the density of the nanofluid, and $M_{nf}=X_{bf}M_{bf}+X_pM_p$ is the molar mass of nanofluid. X_{bf} and X_p are the molar fractions of the base fluid and nanoparticle, respectively, whereas M_{bf} and M_p are the respective molar masses of the base fluid and nanoparticle. The theoretical value of thermal conductivity obtained through the modified Bridgman Eq. (2) is also illustrated in Figure 8.

4 Conclusion

The stable TiO_2-EG nanofluids of various concentrations have been synthesized, and their ultrasonic and thermal properties have been studied at room temperature. The ultrasonic analysis leads to the understanding of the molecular level interactions taking place between the particles and the fluid molecules. The evaluated acoustical parameters clearly confirm that the molecular interaction was pronounced in EG. It was due to the greater association between the solute-solvent molecules in the ethylene solvent. Hence, it has been proven that there had been a strong molecular interaction that existed between the component molecules in the mixtures. In addition, a new approach to find out the thermal conductivity of nanofluids through ultrasonic velocity has been proposed.

Acknowledgments: The authors would like to express their sincere thanks to SAIF, IIT-Madras, Chennai, for providing HRSEM, and the Department of Nuclear Physics, University of Madras, Chennai, for providing the XRD analysis.

References

[1] Shima PD, Philip J. Tuning of thermal conductivity and rheology of nanofluids using an external stimulus. *J. Phys. Chem.* 2011, C 115, 20097–20104.
[2] Das SK, Choi SUS, Yu W, Pradeep T. *Nanofluids: Science and Technology*, John Wiley & Sons, Inc.: Hobokesn, NJ, 2008.
[3] Józefczak A, Hornowski T, Skumiel A. Temperature dependence of particle size distribution in transformer oil-based ferrofluid. *Int. J. Thermophys.* 2011, 32, 795–806.
[4] Wang JJ, Zheng RT, Gao JW, Chen G. Heat conduction mechanisms in nanofluids and suspensions. *Nano Today* 2012, 7, 124–136.
[5] Nagarajan R, Gorai P, Chawla N. Modeling of thermodynamic and transport phenomena in CVD processes for nano-scale applications. *ECS Trans.* 2008, 13, 7–18.
[6] Prasher R, Battacharya P, Phelan PE. Thermal conductivity of nanoscale colloidal solutions (nanofluids). *Phys. Rev. Lett.* 2005, 94, 025901-1–025901-4.
[7] Touloukian YS, Ho CY. *Thermal Properties of Matter*, The TPRC Data Series, Plenum Press: New York, Edn. 1970 to 1977.
[8] Tony J, Krishnakumar TS. Experimental studies of thermal conductivity, viscosity and stability of ethylene glycol nanofluids. *J. IJIRSET* 2013, 2, 611–617.
[9] Maxwell JC. *A Treatise on Electricity and Magnetism*, Vol. 1, 2nd ed., Clarendon Press: Oxford, 1881.
[10] Choi SUS. Enhancing thermal conductivity of fluids with nanoparticles. In *Developments and Applications of Non-Newtonian Flows*, FED-231/MD-66; ASME: New York, 1995, pp. 99–105.
[11] Masuda H, Ebata A, Teramae K, Hishinuma N. Alteration of thermal conductivity and viscosity of liquid by dispersing ultrafine particles. *Netsu Bussei.* 1993, 4, 227–233.
[12] Eastman JA, Choi SUS, Li S, Yu W, Thompson L. Anomalously increased effective thermal conductivities of ethylene-glycol based containing copper nanoparticles. *J. Appl. Phys. Lett.* 2001, 78, 718–720.
[13] Mishra G, Wan M, Pandey V, Singh D, Yadav RR, Mishra B. Ultrasonic and thermal properties of nanofluids containing copper nanoparticles. *IJSR* 2015, 92–95.
[14] Turgut A, Tavman I, Chirtoc M, Schuchmann HP, Sauter C, Tavma S. Thermal conductivity and viscosity measurements of water-based TiO_2 nanofluids. *Int. J. Thermophys.* 2009, 30, 1213–1226.

[15] Das SK, Putra N, Thiesen P, Roetzel W. Temperature dependence of thermal conductivity enhancement for nanofluids. *J. Heat Transfer* 2003, 125, 567–574.
[16] Karthikeyan NR, Philip J, Baldev R. Effect of clustering on the thermal conductivity of nano-fluids. *Mater. Chem. Phys*. 2008, 109, 50–55.
[17] Xie H, Wang J, Xi T, Liu Y, Ai F, Q. Wu. Thermal conductivity enhancement of suspensions containing nanosized alumina particles. *Appl. Phys. Lett.* 2002, 91, 4568–4572.
[18] Chon CH, Kihm KD, Lee SP, Choi SUS. Empirical correlation finding the role of temperature and particle size for nanofluid (Al_2O_3) thermal conductivity enhancement. *Appl. Phys. Lett.* 2005, 87, 153107-1-3.
[19] Jang SP, Choi SUS. Effects of various parameters on nanofluid thermal conductivity. *J. Heat Transfer* 2007, 129, 617–623.
[20] Kim SH, Choi SR, Kim D. Thermal conductivity of metal-oxide nanofluids: particle size dependence and effect of laser irradiation. *J. Heat Transfer* 2007, 129, 298–307.
[21] Hwang YJ, Ahn YC, Shin HS, Lee SG, Kim GT, Park HS, Lee JK. Investigation on characteristics of thermal conductivity enhancement of nanofluids. *Curr. Appl. Phys.* 2006, 6, 1068–1071.
[22] He Y, Jin Y, Chen H, Ding Y, Cang D, Lu H. Heat transfer and flow behavior of aqueous suspensions of TiO_2 nanoparticles (nanofluids) flowing upward through a vertical pipe. *Int. J. Heat Mass Transfer* 2007, 50, 2272–2281.
[23] Wang ZL, Tang DW, Liu S, Zheng XH, Araki N. Thermal-conductivity and thermal-diffusivity measurements of nanofluids by 3-method and mechanism analysis of heat transport. *Int. J. Thermophys.* 2007, 28, 1255–1268.
[24] Murshed SMS, Leong KC, Yang C. Investigations of thermal conductivity and viscosity of nanofluids. *Int. J. Therm. Sci.* 2008, 47, 560–568.
[25] Kiruba R, Gopalakrishnan M, Mahalingam T, Kingson Solomon Jeevaraj A. Ultrasonic studies on zinc oxide nanofluids. *J. Nanofluids* 2012, 1, 97–100.
[26] Nabeel Rashin M, Hemalatha J. Acoustic study on the interactions of coconut oil based copper oxide nanofluid. *Int. J. Eng. Appl. Sci.* 2012, 6, 216–220.
[27] Hemalatha J, Prabhakaran T, Nalini RP. A comparative study on particle–fluid interactions in micro and nanofluids of aluminium oxide. *Microfluid Nanofluidics* 2011, 10, 263–270.
[28] Sastry NV, Patel MC. Densities, excess molar volumes, viscosities, speeds of sound, excess isentropic compressibilities, and relative permittivities for alkyl (methyl, ethyl, butyl, and isoamyl) acetates + glycols at different temperatures. *J. Chem. Eng. Data* 2003, 48, 1019–1027.
[29] Zhao Y, Li C, Liu X, Gu F, Jiang H, Shao W, Zhang L, He Y. Synthesis and optical properties of TiO_2 nanoparticles. *Mater. Lett.* 2007, 61, 79–83.
[30] Madhusudan Reddy K, Manorama S V, Ramachandra Reddy A. Bandgap studies on anatase titanium dioxide nanoparticles. *Mater. Chem. Phys*. 2002, 78, 239–245.
[31] Nabeel Rashin M, Hemalatha J. A novel ultrasonic approach to determine thermal conductivity in CuO-EG nanofluids. *J. Mol. Liq.* 2014, 197, 257–262.
[32] Harish S, Ishikawa K, Einarsson E, Aikawa S, Chiashi S, Shiomi J, Maruyama S. Enhanced thermal conductivity of ethylene glycol with single-walled carbon nanotube inclusions. *Int. J. Heat Mass Transfer* 2012, 55, 3885–3890.
[33] Prasher R, Phelan PE, Bhattacharya P. Effect of aggregation kinetics on the thermal conductivity of nanoscale colloidal solutions (nanofluid). *Nano Lett.* 2006, 6, 1529–1534.
[34] Philip J, Shima PD. Thermal properties of nanofluids. *Adv. Colloid Interface Sci.* 2012, 183–184, 30–35.
[35] Debye P. Angular dissymmetry of the critical opalescence in liquid mixtures. *J. Chem. Phys*. 1959, 31, 680–687.
[36] Bird RB, Stewart WE, Lightfoot EN. *Transport Phenomena*, John Wiley & Sons: New York, 2011, pp. 65.